SCIENTIFIC REPORTS

OPEN

SUBJECT AREAS:
CHEMISTRY
MATERIALS CHEMISTRY
NANOTECHNOLOGY
SYNTHESIS

Received
6 May 2011

Accepted
17 June 2011

Published
30 June 2011

Correspondence and requests for materials should be addressed to Y.S. (shimak@scl.kyoto-u.ac.jp)

Selective reduction of layers at low temperature in artificial superlattice thin films

Kazuya Matsumoto[1], Mitsutaka Haruta[1], Masanori Kawai[1], Aya Sakaiguchi[1], Noriya Ichikawa[1], Hiroki Kurata[1] & Yuichi Shimakawa[1,2]

[1]Institute for Chemical Research, Kyoto University, Uji, Kyoto 611-0011, Japan, [2]Japan Science and Technology Agency, CREST, Uji, Kyoto 611-0011, Japan.

Reduction and oxidation in transition-metal oxides are keys to develop technologies related to energy and the environment. Here we report the selective topochemical reduction observed when artificial superlattices with transition-metal oxides are treated at a temperature below 300 °C with CaH_2. $[CaFeO_2]_m/[SrTiO_3]_n$ infinite-layer/perovskite artificial superlattice thin films were obtained by low-temperature reduction of $[CaFeO_{2.5}]_m/[SrTiO_3]_n$ brownmillerite/perovskite artificial superlattice thin films. By the reduction only the $CaFeO_{2.5}$ layers in the artificial superlattices were reduced to the $CaFeO_2$ infinite layers whereas the $SrTiO_3$ layers were unchanged. The observed low-temperature reduction behaviors strongly suggest that the oxygen ion diffusion in the artificial superlattices is confined within the two-dimensional brownmillerite layers. The reduced artificial superlattice could be reoxidized, and thus, the selective reduction and oxidation of the constituent layers in the perovskite-structure framework occur reversibly.

Oxygen-deficient perovskites $AFeO_{3-\delta}$ (A = Sr or Ca) ($\delta = 0 \sim 1.0$) attract much attention because they show wide varieties in crystal structures and physical properties as a function of oxygen content, and thus they have been studied extensively for more than 40 years[1–4]. For example, $SrFeO_3$ ($\delta = 0$) is a simple perovskite, contains iron ions with unusually high valence state (Fe^{4+}), which is stabilized by a strong oxidizing atmosphere, and exhibits metallic conductivity[1,5,6]. $SrFeO_{2.5}$ ($\delta = 0.5$), on the other hand, is synthesized at an ambient condition, and its brownmillerite structure consists of alternate layers of Fe^{3+} octahedra and tetrahedra, and is an antiferromagnetic insulator[7]. Although it was not possible to produce a perovskite with Fe^{2+} by using any reduction techniques, recently low-temperature topochemical reduction made the brownmillerite $SrFeO_{2.5}$ to an infinite-layer structure $SrFeO_2$ ($\delta = 1.0$)[8–10]. Such a wide range of oxygen nonstoichiometry could also be exploited in applications for electrochemical energy generation and storage devices[11–13].

The infinite-layer structure $AFeO_2$ is the first iron oxide with Fe^{2+} with an unusual square-planar coordination of oxygen, and is made from the corresponding brownmillerite $AFeO_{2.5}$ by reducing it at a low temperature with CaH_2 (refs. 8 and 14). This reduction reaction changes the iron from Fe^{3+} with a tetrahedral or octahedral coordination to Fe^{2+} with an unusual square-planar coordination[15]. A similar reaction with CaH_2 also reduces a perovskite $LaNiO_3$ to an infinite-layer structure $LaNiO_2$ with unusual square-planar coordinated monovalent Ni (refs. 16–18). Thus, the low-temperature reduction removes oxygen atoms from the fundamental perovskite-structure framework and adjusts the oxidation state and the oxygen coordination of cations[19,20].

$AFeO_2$ is also obtained in a single-crystalline thin film form by the reduction of $AFeO_{2.5}$ thin film[21,22]. Interestingly, the topotactic reduction of thin films of the brownmillerite $CaFeO_{2.5}$ to the infinite-layer $CaFeO_2$ revealed that there are two ways of oxygen rearrangement that have different kinetics. Both a-axis oriented and b-axis oriented $CaFeO_{2.5}$ thin films changed to the c-axis oriented $CaFeO_2$ films, but the complete reduction of the b-axis oriented film took longer time than that of the film oriented on the a axis[23]. Thus, the low-temperature reduction behaviors seen in the thin film samples provide us deep insight into oxygen-ion rearrangement in oxides.

Similar oxygen release and rearrangement were seen in the reduction of an artificial brownmillerite superlattice thin film consisting of $CaFeO_{2.5}$ and $SrFeO_{2.5}$ to an infinite-layer-structure superlattice thin film consisting of $CaFeO_2$ and $SrFeO_2$ (ref. 24). The oxygen atoms in the constituent brownmillerite-structure oxides are released from the superlattice layers of the thin film. This raised an interesting question as to what happens during the

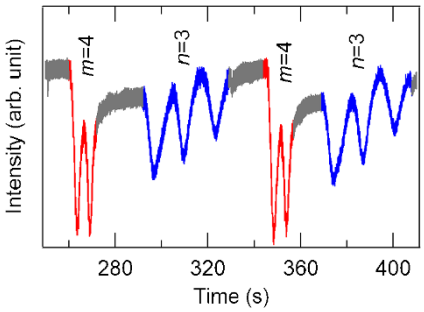

Figure 1 | RHEED intensity oscillations during deposition. RHEED intensity oscillations during the growth of a $[CaFeO_{2.5}]_4/[SrTiO_3]_3$ superlattice on a $SrTiO_3$ (001) substrate. Red and blue oscillations correspond to the growth of $[CaFeO_{2.5}]_4$ and $[SrTiO_3]_3$, respectively.

reduction of artificial superlattice thin films consisting of the brownmillerite $CaFeO_{2.5}$ and the perovskite $SrTiO_3$. Because $SrTiO_3$ is rather stable in any atmosphere, the oxygen rearrangement facilities are expected to be different between the two constituent layers. The reduction behaviors of such artificial superlattices are investigated in the work reported here.

Results

Brownmillerite/perovskite artificial superlattices, $[CaFeO_{2.5}]_m/[SrTiO_3]_n$ (m = 4, 6, and 8; n = 1, 2, 3, and 4), were prepared on single-crystal $SrTiO_3$(001) substrates by pulsed laser deposition. The reflection high energy electron diffraction (RHEED) intensity oscillation during the growth of a $[CaFeO_{2.5}]_4/[SrTiO_3]_3$ superlattice is shown in Fig. 1. The observed clear oscillation pattern confirms that both $CaFeO_{2.5}$ and $SrTiO_3$ are grown in a layer-by-layer growth mode. As reported in a previous paper[24], *b*-axis-orientated $[CaFeO_{2.5}]_2$ 7.4 Å thick, a thickness corresponding to one FeO_6 octahedron and one FeO_4 tetrahedron, grew during a single RHEED oscillation. Thus, the deposition of $CaFeO_{2.5}$ for the two oscillations produces m = 4 layers. One-unit-cell-thick $SrTiO_3$ (3.91 Å) can also be deposited during a single RHEED oscillation.

As shown in the X-ray diffraction pattern of the $[CaFeO_{2.5}]_4/[SrTiO_3]_1$ superlattice in Fig. 2a (the structure model is shown in Fig. 2b), the (0 0 *l*) diffraction peaks confirm the successful growth of the superlattice structure. Note that the stacking direction of the artificial superlattice is defined here as the *c* direction. The X-ray diffraction patterns of the m = 8 (n = 1, 2, 3, and 4) and m = 6 (n = 1, 2, 3, and 4) superlattices prepared in the present study are also shown in Supplementary Figs. S1 and S2, respectively. As shown in Fig. 3, the out-of-plane lattice constants of the as-deposited $[CaFeO_{2.5}]_m/[SrTiO_3]_n$ brownmillerite/perovskite superlattices are on the line of 3.70 [= *b* ($CaFeO_{2.5}$: 14.8 Å)/4] × m + 3.91 × n Å. These results thus clearly show that the brownmillerite/perovskite superlattices were prepared as designed.

The films were then treated, in evacuated glass tubes, with CaH_2 at 280 °C for 48 h. After the reduction process, the (0 0 *l*) peak positions of the thin films in the X-ray diffraction patterns changed to higher angles (see Fig. 2a, and Supplementary Figs. S1 and S2), and thus the out-of-plane lattice constants decreased significantly. The 18.9 Å out-of-plane lattice constant of the as-deposited m=4 and n=1 film, for example as seen in Fig. 2a, decreased to 17.9 Å. What is of particular interest here is that the reduced out-of-plane lattice constant is very close to the lattice constant of an artificial superlattice, which consists of four unit cells of the infinite-layer-structure $CaFeO_2$ and one unit cell of $SrTiO_3$. The observed diffraction intensities shown in Fig. 2a are also consistent with those simulated for the superlattice structure model with the infinite-layer $CaFeO_2$ and the perovskite $SrTiO_3$ shown in Fig. 2c.

The reduction of the $CaFeO_{2.5}$ brownmillerite layer to the infinite-layer structure $CaFeO_2$ in the superlattice was also confirmed by a cross-sectional high-angle annular dark-field scanning transmission electron microscope (HAADF-STEM) image shown in Fig. 4. Although the four-coordinated Fe and six-coordinated Fe in the brownmillerite structure are distinguishable in the HAADF-STEM image (see inset of Fig. 4), such features are not evident in the reduced superlattice, suggesting that all Fe in the reduced film are square-planar coordinated by oxygen ions. The alternate stacking of eight layers of $CaFeO_2$ and three layers $SrTiO_3$ is clearly seen with sharp interfaces. It should also be noted that the bright Sr column distances in the image of the $SrTiO_3$ layer in the reduced film do not change from those of the as-deposited $SrTiO_3$. This implies that no significant oxygen deficiencies are introduced in the $SrTiO_3$ layers after the low-temperature reduction.

The out-of-plane lattice constants of all the reduced superlattices can be fitted with the formula 3.35 [=*c* ($CaFeO_2$)] × m + 3.91 × n Å. As shown in Fig. 3, the reduction in the out-of-plane lattice constant always corresponds to the thickness decrease due to the change from brownmillerite $CaFeO_{2.5}$ to infinite-layer $CaFeO_2$. It is thus clear that the reduced superlattices consist of the infinite-layer $CaFeO_2$ and the perovskite $SrTiO_3$ and that only the brownmillerite $CaFeO_{2.5}$ layers were reduced by the low-temperature annealing (see the structure in Fig. 2c). The result is completely different from the reduction of the

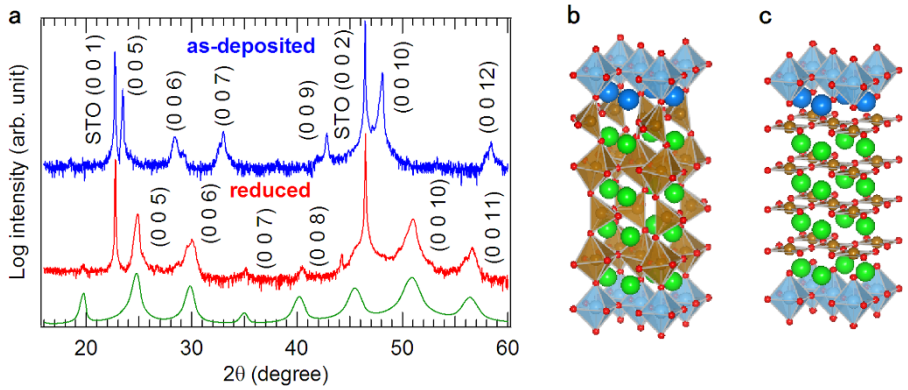

Figure 2 | XRD patterns and crystal structures of artificial superlattices. (a) X-ray diffraction patterns of the as-deposited $[CaFeO_{2.5}]_4/[SrTiO_3]_1$ brownmillerite/perovskite superlattice and the reduced $[CaFeO_2]_4/[SrTiO_3]_1$ infinite-layer/perovskite superlattice. Also shown at the bottom is the X-ray diffraction pattern calculated from the superlattice structure model of $[CaFeO_2]_4/[SrTiO_3]_1$ shown in Figure 2c. (b), (c) Crystal structures of (b) the $[CaFeO_{2.5}]_4/[SrTiO_3]_1$ brownmillerite/perovskite superlattice and (c) the reduced $[CaFeO_2]_4/[SrTiO_3]_1$ infinite-layer/perovskite superlattice. The brownmillerite and infinite-layer structures are drawn with Ca in green, Fe in brown, and O in red, and the perovskite structure is drawn with Sr in blue and TiO_6 octahedra in light blue.

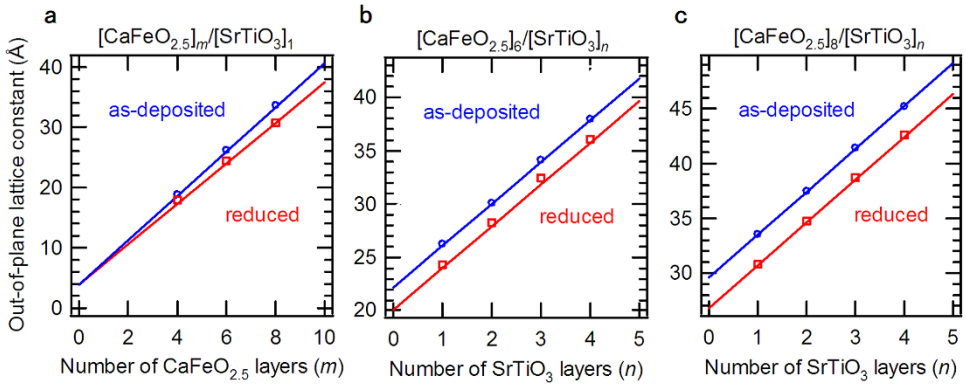

Figure 3 | Out-of-plane lattice constants of as-deposited and reduced artificial superlattices. (a) Relation between the number m of $CaFeO_{2.5}$ layers and the out-of-plane lattice constants of (○) as-deposited and (□) reduced $[CaFeO_{2.5}]_m/[SrTiO_3]_1$ brownmillerite/perovskite superlattices. The lattice constants of the as-deposited superlattices fit the blue line ($3.70\times m + 3.91$) and those of the reduced superlattices fit the red line ($3.35\times m + 3.91$). (b) Relation between the number n of $SrTiO_3$ layers and the out-of-plane lattice constants of (○) as-deposited and (□) reduced $[CaFeO_{2.5}]_6/[SrTiO_3]_n$ brownmillerite/perovskite superlattices. The lattice constants of the as-deposited superlattices fit the blue line ($3.70\times 6 + 3.91\times n$) and those of the reduced superlattices fit the red line ($3.35\times 6 + 3.91\times n$). (c) Same as (b) but for $[CaFeO_{2.5}]_8/[SrTiO_3]_n$ superlattices. The out-of-plane lattice constants of the as-deposited and reduced films follow ($3.70\times 8 + 3.91\times n$) and ($3.35\times 8 + 3.91\times n$), respectively.

$[CaFeO_{2.5}]/[SrFeO_{2.5}]$ superlattice, in which both constituent brownmillerite $CaFeO_{2.5}$ and $SrFeO_{2.5}$ layers were reduced to the infinite-layer structures.

Discussion

Transition-metal ions are well known to show variation in their oxidation states. The oxidation states of Fe, for example, are typically 2+ and 3 +, and those of Ti are 2+, 3+, and 4+. The present results with the $[CaFeO_{2.5}]/[SrTiO_3]$ artificial superlattices clearly show that the Fe^{3+} in the $CaFeO_{2.5}$ brownmillerite is reduced to Fe^{2+} whereas Ti^{4+} in $SrTiO_3$ is not reduced under the same reducing atmosphere with CaH_2. This is, of course, related to the difference in reduction facilities between Fe^{3+} (the third ionization energy; 30.6 eV) and Ti^{4+} (the fourth ionization energy; 43.3 eV). In addition, octahedral coordination with oxygen ions for Ti^{4+} is pretty stable, but square planar and tetrahedral coordinations are difficult to stabilize.

The results thus suggest the difference in oxygen rearrangement facilities between the two constituent layers and also raise interesting discussion as to how the oxygen atoms are released and rearranged in the present brownmillerite/perovskite superlattices. In the reduction process, if we assume that the oxygen ions are released mainly from the film surface, the results appear to imply that the oxygen ions pass through the perovskite $SrTiO_3$ layers. Considering the fairly large lateral size of the film samples (5 mm × 5 mm × 70 nm-thick), this oxygen diffusion process is possible. In the brownmillerite structure the oxygen ions travel by way of atomic vacancy sites, whereas in the perovskite $SrTiO_3$ structure they travel by way of exchange reactions in the octahedron. On the other hand, suppose that the oxygen ions are released mainly from the sides of the film sample, the oxygen ions travel within the two-dimensional brownmillerite layers, instead of passing through the $SrTiO_3$ layers.

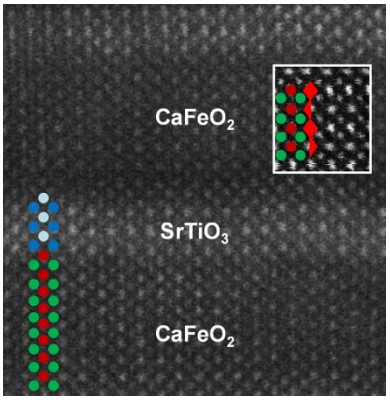

Figure 4 | HAADF-STEM image of reduced artificial superlattice thin film. HAADF-STEM image of the reduced $[CaFeO_2]_8/[SrTiO_3]_3$ superlattice. The blue, sky blue, green, and red spheres respectively represent Sr, Ti, Ca, and Fe atoms. Inset shows a typical HAADF-STEM image of brownmillerite $CaFeO_{2.5}$, where FeO_6 octahedra and FeO_4 tetrahedra are distinguishable as illustrated on the image.

Note here that the time required for the complete reduction of the brownmillerite/perovskite superlattices is almost the same irrespective of the thickness of $SrTiO_3$ layers. Although the actual oxygen diffusion should occur along both perpendicular and parallel directions of the films and the dominant diffusion process may depend on the reduction temperature, the present results strongly suggest that the oxygen diffusion through the thin $SrTiO_3$ layer is not the main pathway at 280 °C. Therefore, at low temperatures like 280 °C, the stable $SrTiO_3$ layers can act as barriers for the oxygen diffusion and the oxygen ion diffusion is confined within the two-dimensional brownmillerite layers. It was indeed reported that the coherent interface in epitaxial ZrO_2:Y_2O_3/$SrTiO_3$ heterostructures increased oxygen mobility at room temperature[25–27]. This suggests that the specific two-dimensional structural feature has important roles in oxygen diffusion in solids, especially at low temperatures.

The reduced infinite-layer/perovskite artificial superlattice could be reoxidized to the brownmillerite/perovskite superlattice by annealing it in an oxidizing atmosphere. Oxygen atoms could be released selectively from the brownmillerite layers and also incorporated into the infinite-layer structure. Thus, the selective reduction and oxidation in the perovskite-structure framework occur reversibly. The results also give a potential application of the artificial superlattice as a two-dimensional oxygen reservoir.

In conclusion, $[CaFeO_2]_m/[SrTiO_3]_n$ infinite-layer/perovskite superlattices were prepared by low-temperature reduction of $[CaFeO_{2.5}]_m/[SrTiO_3]_n$ brownmillerite/perovskite superlattices. The brownmillerite/perovskite superlattices were made by pulsed laser deposition in a layer-by-layer growth mode by monitoring the RHEED intensity oscillation during the deposition. The structure analysis of X-ray diffraction data and the HAADF-STEM observation confirmed the successful reduction of the films to the infinite-layer/perovskite superlattices. By the low-temperature reduction with CaH_2, only the brownmillerite $CaFeO_{2.5}$ layers were

reduced to the infinite-layer structure $CaFeO_2$ in the superlattices whereas the $SrTiO_3$ layers were unchanged. The results strongly suggest that, in the low-temperature reduction of the $[CaFeO_{2.5}]/[SrTiO_3]$ artificial superlattices, the stable $SrTiO_3$ layers can act as barriers for the oxygen diffusion and the oxygen ion diffusion is confined within the two-dimensional brownmillerite layers.

Methods

The artificial superlattice thin films were prepared from $CaFeO_{2.5}$ and $SrTiO_3$ ceramic targets by pulsed laser deposition using a KrF excimer laser pulse ($\lambda = 248$ nm) (COHERENT COMPex-Pro 205 F). The polycrystalline brownmillerite $CaFeO_{2.5}$ was synthesized by solid-state reaction of Fe_2O_3 and $CaCO_3$ at 1200 °C for 36 h in air. Brownmillerite/perovskite superlattices, $[CaFeO_{2.5}]_m/[SrTiO_3]_n$ (m = 4, 6, and 8; n = 1, 2, 3, and 4), were prepared on single-crystal $SrTiO_3$(001) substrates with atomically flat terraces and unit-cell steps. The deposition started with $CaFeO_{2.5}$, and then $SrTiO_3$ was deposited. The oxygen partial pressure during the depositions was 10^{-5} Torr, and the substrate temperature was monitored with a pyrometer and kept at 600 °C.

The thickness of each layer was controlled by *in situ* observation of reflection high energy electron diffraction (RHEED) intensity oscillation, and the total thickness of the artificial superlattice was checked by measuring the Raue fringes in X-ray diffraction profiles and by measuring the X-ray reflectivity of the film. The deposited artificial superlattice thin films were embedded with about 0.25 g CaH_2 powder in glass tubes in an argon-filled glove box and the tubes were sealed under vacuum conditions, after which they were kept at 280 °C for 48h. The residual products and unreacted CaH_2 on the film surface were removed by rinsing in 2-butanone.

The structures of the superlattices were evaluated by 2θ-θ X-ray diffraction measurements with Cu $K\alpha$ radiation (PANalytical X'Pert MRD) and the observed diffraction intensities for the artificial superlattice thin films were compared to the calculated ones by the simulation program RIETAN-2000[28]. The structures were also studied by cross-sectional high-angle annular dark-field scanning transmission electron microscope (HAADF-STEM) observations with a JEM-9980TKP1.

1. MacChesney, J. B., Sherwood, R. C. & Potter, J. F. Electric and magnetic properties of the strontium ferrates. *J. Chem. Phys.* **43**, 1907–1913 (1965).
2. Takeda, Y. *et al.* Phase relation in the oxygen nonstoichiometric system, $SrFeO_x$ ($2.5 \leq x \leq 3.0$). *J. Solid State Chem.* **63**, 237–249 (1986).
3. Hodges, J. P. *et al.* Evolution of oxygen-vacancy ordered crystal structures in the perovskite series $Sr_nFe_nO_{3n-1}$ (n=2, 4, 8, and ∞), and the relationship to electronic and magnetic properties. *J. Solid State Chem.* **151**, 190–209 (2000).
4. Woodward, P. M., Cox, D. E., Moshopoulou, E., Sleight, A. W. & Morimoto, S. Structural studies of charge disproportionation and magnetic order in $CaFeO_3$. *Phys. Rev. B* **62**, 844–855 (2000).
5. Hayashi, N., Terashima, T. & Takano, M. Oxygen-holes creating different electronic phases in Fe^{4+}-oxides: Successful growth of single crystalline films of $SrFeO_3$ and related perovskites at low oxygen pressure. *J. Mater. Chem.* **11**, 2235–2237 (2001).
6. Lebon, A. *et al.* Magnetism, charge order, and giant magnetoresistance in $SrFeO_{3-\delta}$ single crystals. *Phys. Rev. Lett.* **92**, 037202 (2004).
7. Schmidt, M. & Campbell, S. J. Crystal and magnetic structures of $Sr_2Fe_2O_5$ at elevated temperature. *J. Solid State Chem.* **156**, 292–304 (2001).
8. Tsujimoto, Y. *et al.* Infinite-layer iron oxide with a square-planar coordination. *Nature* **450**, 1062–1065 (2007).
9. Kohler, J. Square-planar coordinated iron in the layered oxoferrate(II) $SrFeO_2$. *Angew. Chem. Int. Ed.* **47**, 4470–4472 (2008).
10. Tassel, C. *et al.* Stability of the infinite layer structure with iron square planar coordination. *J. Am. Chem. Soc.* **130**, 3764–3765 (2008).
11. Sammells, A. F., Schwartz, M., Mackay, R. A., Barton, T. F. & Peterson, D. R. Catalytic membrane reactors for spontaneous synthesis gas production. *Catal. Today* **56**, 325–328 (2000).
12. Badwal, S. P. S. & Ciacchi, F. T. Ceramic membrane technologies for oxygen separation. *Adv. Mater.* **13**, 993–996 (2001).
13. Shao, Z. & Haile, S. M. A high-performance cathode for the next generation of solid-oxide fuel cells. *Nature* **431**, 170–173 (2004).
14. Tassel, C. *et al.* $CaFeO_2$: A new type of layered structure with iron in a distorted square planar coordination. *J. Am. Chem. Soc.* **131**, 221–229 (2009).
15. Hayward, M. A. & Rosseinsky, M. J. Materials chemistry: Cool conditions for mobile ions. *Nature* **450**, 960–961 (2007).
16. Hayward, M. A., Green, M. A., Rosseinsky, M. J. & Sloan, J. Sodium hydride as a powerful reducing agent for topotactic oxide deintercalation: Synthesis and characterization of the nickel(I) oxide $LaNiO_2$. *J. Am. Chem. Soc.* **121**, 8843–8854 (1999).
17. Kawai, M. *et al.* Reversible changes of epitaxial thin films from perovskite $LaNiO_3$ to infinite-layer structure $LaNiO_2$. *Appl. Phys. Lett.* **94**, 082102 (2009).
18. Kawai, M. *et al.* Orientation change of an infinite-layer structure $LaNiO_2$ epitaxial thin film by annealing with CaH_2. *Cryst. Growth Des.* **10**, 2044–2046 (2010).
19. Hayward, M. A. & Rosseinsky, M. J. Anion vacancy distribution and magnetism in the new reduced layered Co(II)/Co(I) phase $LaSrCoO_{3.5-x}$. *Chem. Mater.* **12**, 2182–2195 (2000).
20. Hadermann, J., Abakumov, A. M., Adkin, J. J. & Hayward, M. A. Topotactic reduction as a route to new close-packed anion deficient perovskites: Structure and magnetism of 4H-$BaMnO_{2+x}$. *J. Am. Chem. Soc.* **131**, 10598–10604 (2009).
21. Inoue, S. *et al.* Single-crystal epitaxial thin films of $SrFeO_2$ with FeO_2 "infinite layers". *Appl. Phys. Lett.* **92**, 161911 (2008).
22. Shimakawa, Y. *et al.* Topotactic changes in thin films of brownmillerite $SrFeO_{2.5}$ grown on $SrTiO_3$ substrates to infinite-layer structure $SrFeO_2$. *Cryst. Growth Des.* **10**, 4713–4715 (2010).
23. Inoue, S. *et al.* Anisotropic oxygen diffusion at low temperature in perovskite-structure iron oxides. *Nat. Chem.* **2**, 213–217 (2010).
24. Matsumoto, K. *et al.* Artificial superlattice thin film of infinite-layer structure $[CaFeO_2]/[SrFeO_2]$. *Appl. Phys. Express* **3**, 105601 (2010).
25. Garcia-Barriocanal, J. *et al.* Colossal ionic conductivity at interfaces of epitaxial ZrO_2:Y_2O_3/$SrTiO_3$ heterostructures. *Science* **321**, 676–680 (2008).
26. Kilner, J. A. Ionic conductors: Feel the strain. *Nat. Mater.* **7,** 838–839 (2008).
27. Guo, X. & Maier, J. Ionically conducting two-dimensional heterostructures. *Adv. Mater.* **21**, 2619–2631 (2009).
28. Izumi, F. & Ikeda, T. A Rietveld-analysis program RIETAN-98 and its applications to zeolites. *Mater. Sci. Forum* **321–324**, 198–203 (2000).

Acknowledgements

We thank S. Inoue and S. Isoda for discussions. This work was supported in part by a Grant-in-Aid for Scientific Research 19GS0207, by the Global Centers of Excellence Program "International Center for Integrated Research and Advanced Education in Materials Science", and by a grant for the Joint Project of Chemical Synthesis Core Research Institutions from the Ministry of Education, Culture, Sports, Science and Technology of Japan. The work was also supported by Japan Science and Technology Agency, CREST.

Author contributions

K.M. and Y.S. conceived and designed the study. K.M. and M.K. performed the experiments with the help of A.S. and N.I. M.H. and H.K. made the HAADF-STEM observation. All of the authors discussed the results. K.M. and Y.S. wrote the manuscript.

Additional information

Supplementary Information accompanies this paper at http://www.nature.com/scientificreports

Competing financial interests: The authors declare no competing financial interests.

How to cite this article: Matsumoto, K. *et al.* Selective reduction of layers at low temperature in artificial superlattice thin films. *Sci. Rep.* **1**, 27; DOI:10.1038/srep00027 (2011).